Monitoring General Linear Profiles Using Multivariate EWMA schemes

Changliang Zou
Department of Statistics
School of Mathematical Sciences
Nankai University
Tianjian, PR China

Fugee Tsung
Department of Industrial Engineering
and Logistics Management
Hong Kong University of Science and
Technology
Clear Water Bay, Kowloon, Hong Kong

Zhaojun Wang
Department of Statistics
School of Mathematical Sciences
Nankai University
Tianjian, PR China
LPMC of China
(zjwang@nankai.edu.cn)

Abstract

We propose a statistical process control (SPC) scheme that can be implemented in industrial practice, where the quality of a process can be characterized by a general linear profile. We start by reviewing the general linear profile model and the existing monitoring methods. Based on that, a novel multivariate exponentially weighted moving average monitoring (MEWMA) scheme is proposed for such a profile. Three enhancement features are introduced to further improve the performance of the proposed scheme, which include 1) the variable sampling interval, 2) the self-starting function, and 3) the parametric diagnostic approach. Throughout this paper, a deep reactive ion etching (DRIE) example from semiconductor manufacturing, which has a profile that fits a quadratic polynomial regression model well, is used to illustrate the implementation of the proposed approach.

1 Introduction

Statistical process control (SPC) has been widely used to monitor various industrial processes. Most SPC applications assume that the quality of a process can be adequately represented by the distribution of a quality characteristic. However, in many situations, the quality of a process may be better characterized and summarized by a relationship between the response variable and one or more explanatory variables. That is, the focus would be on monitoring the profile that represents such a relationship, instead of on monitoring a single characteristic. Among others, studies focusing on linear profiles have been particularly influential. See, for example, Jensen *et al.* (1984), Mestek *el al.* (1994), Stover and Brill (1998), Lawless *et al.* (1999) and Kang and Albin (2000).

Kang and Albin (2000) proposed two control charts for Phase II monitoring of simple linear profiles. One of these is a multivariate T^2 chart and the other is a combination of an exponentially weighted moving average (EWMA) chart to monitor the regression residuals and a range (R) chart to monitor the standard deviations. Kim *et al.* (2003) proposed a method based on the combination of three EWMA charts. Instead of using deviations from the in-control process center, they coded the independent variable so that the average value was zero and used the estimated regression coefficients from each sample, i.e., the estimates of the Y-intercept and slope, to construct two univariate EWMA charts. Another one-sided EWMA chart was then used to monitor the increases in standard deviation of the process. Gupta *et al.* (2006) compared the performance of two phase II monitoring schemes of linear profiles, the control charting schemes proposed by Croarkin and Varner (1982) and Kim *et al.* (2003). Their simulation study showed that Croarkin and Varner's method (1982) performed poorly compared to Kim *et al.*'s (2003) combined control charting scheme. Mahmoud and Woodall (2004) studied the Phase I method for monitoring the linear profiles. Following that, Mahmoud *et al.* (2005) proposed a change-point method, based on the likelihood ratio statistics, to detect sustained changes in a linear profile data set in Phase I. Zou *et al.* (2006) proposed a control chart based on change-point model for monitoring linear profiles for which the parameters are unknown but may be estimated from historical samples. A extensive discussion of research problems in monitoring linear profiles can be found

in Woodall *et al.* (2004).

All these recent studies concentrated on the situation with a simple linear profile that can be adequately represented by a straight line. Although such a simple linear profile can characterize various applications as in the literature, general linear profiles that include both a polynomial regression and a multiple linear regression relationship may be even more representative of most industrial applications. However, research on monitoring and diagnosis of general linear profiles is still scanty. In this paper, we focus on a study of the Phase II method for monitoring a general linear profile that can be represented by a polynomial regression or a multiple linear regression relationship. We propose utilizing a multivariate exponentially weighted moving average (MEWMA) scheme (Lowry *et al.* (1992)) for the transformations of estimated parameters, as a single chart to monitor both the coefficients and variance of a general linear profile. The complexity of the proposed single chart approach will not increase as the profile parameters increase as in the existing multiple chart approaches in most of the literature. Also, this chart can be designed and constructed easily and has rather satisfactory performance. In addition, the proposed MEWMA scheme for general linear profiles can be enhanced by the following three features: (1) we enhance the proposed charting scheme with variable sampling interval (VSI) features to improve the efficiency of detecting profile changes; (2) we add a self-starting feature to the proposed chart for situations with unknown parameters or short-run productions where complete Phase I modeling is not feasible; (3) we provide a systematic diagnostic approach to identify the location of the change and to determine which parameters in the profile have changed.

The remainder of this paper is organized as follows: in Section 2, we introduce the deep reactive ion etching (DRIE) example from semiconductor manufacturing that motivates this research. After that, the general linear profile model and the existing monitoring methods such as Kim *et al.* (2003) are reviewed in Section 3. In Section 4, our proposed MEWMA schemes are presented. The proposed chart with the VSI feature is presented in Section 5. The average run length (ARL) and average time to signal (ATS) calibrations of the proposed chart are discussed in Section 6. Based on those results, the monitoring performance of the proposed scheme is compared with that of existing methods in Section 7. A systematic approach for profile diagnosis

is provided in Section 8, which is critical for a more complicated general linear profile. After that, the performance assessments of the estimates of change-points and the identification of special causes are also reported. A self-starting control scheme enhancement is proposed in Section 9 to deal with the cases with unknown parameters and short-run productions. The motivated DRIE example, which has a profile that fits a quadratic polynomial regression model well, is used to illustrate the implementation of the proposed approach step by step in Section 10. Section 11 concludes this paper by summarizing its contributions and suggesting some future research. Some derivations are detailed in the Appendix.

2 The Motivating Example: Monitoring a Deep Reactive Ion Etching Process

We use a micro-electro-mechanical systems (MEMS) fabrication example taken from semiconductor manufacturing to illustrate the motivation for this research. In particular, the deep reactive ion etching (DRIE) process is selected, because it is a key operation in MEMS fabrication to form desired patterns on semiconductor wafers, and it requires careful control and monitoring on a run-to-run basis.

The DRIE process involves complex chemical-mechanical reactions on a machine called an inductive coupled plasma (ICP) silicon etcher made by Surface Technology System Ltd. (STS) (see McAuley *et al.* (2001), Rauf *et al.* (2002) and Zhou *et al.* (2004) for more details about this system). A schematic diagram of such a system is provided in the appendix. The central part of the machine is a process chamber, within which wafers are loaded and processed. The system first releases etching plasma into the chamber to etch trenches following a designed mask pattern, then, in the deposition step, different gases are introduced into the chamber to generate a protective film on the sidewalls. The etching and deposition steps are repeated alternately until a preset processing time is reached, or the end point detection module confirms the correct etching depth.

In the DRIE process, the quality measurement of an etched wafer is conducted with a scanning electron microscope (SEM) in laboratories, and one of the most important quality characteristics is the profile of a trench that may significantly

impact the downstream operations (May *et al.* (1991)). The desired profile is the one with smooth and vertical sidewalls as indicated in center sample of Figure 1, which is called the anisotropic profile. Ideally, the sidewalls of a trench are perpendicular to the bottom of the trench with certain degrees of smoothness around the corners. Various shapes of profile, such as positive and negative profiles, which are due to under-etching and over-etching, are considered to be unacceptable (see Figure 1).

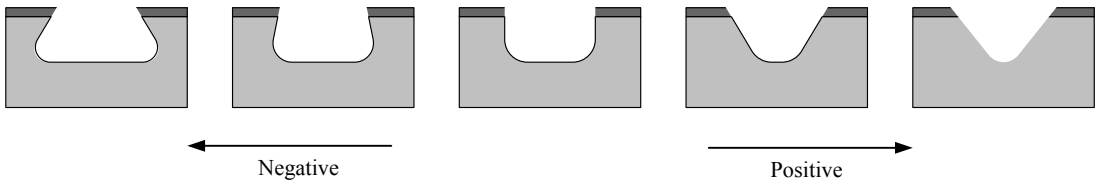

Figure 1: Illustrations of various etching profiles from a DRIE process.

Current industrial practice is to monitor the angles of the sidewalls. Although the sidewall angle is easier to measure, it is known to contain incomplete information about the trench profile, and, in many cases, it may not differentiate various out-of-control profiles. Although it is natural to consider directly monitoring the profile of the trench, which may give more complete information for effective monitoring and diagnosis, exactly how to implement SPC monitoring of a DRIE profile, which apparently cannot be modeled as a straight line, still remains a challenge. In the remainder of this paper, we propose an SPC scheme to monitor such a profile and give a step-by-step demonstration of how to implement the proposed scheme in practice in a later section.

3 The General Linear Profile Model and Existing Monitoring Schemes

In this section we describe the modeling of a general linear profile and review the existing profile monitoring schemes in the literature.

Assume that for the jth random sample collected over time, we have the observations $(\mathbf{X}_j, \mathbf{Y}_j)$, where $\mathbf{Y}_j$ is n_j-variate vector and $\mathbf{X}_j$ is a $n_j \times p$ $(n_j > p)$ matrix.

It is assumed that when the process is in statistical control, the underlying model is

$$\mathbf{Y}_j = \mathbf{X}_j\beta + \varepsilon_j, \tag{1}$$

where $\beta = (\beta^{(1)}, \beta^{(2)}, \cdots, \beta^{(p)})$ is the p-dimensional coefficient vector and the ε_js are i.i.d as a n_j-variate multivariate normal random vector with mean zero and $\sigma^2\mathbf{I}$ covariance matrix. Without loss of generality, here suppose that $\mathbf{X}_j$ is of form $(\mathbf{1}, \mathbf{X}_j^*)$, where $\mathbf{X}_j^*$ is orthogonal to $\mathbf{1}$ and $\mathbf{1}$ is a p-variate vector of all 1s. Otherwise, we can obtain such a form through some appropriate transformations. The n_js are usually equal (denoted as n) and the explanatory variable, $\mathbf{X}_j$, is assumed to be fixed for different j (denoted as $\mathbf{X}$). This is usually the case in practical calibration applications and is also consistent with Kang and Ablin (2000), Kim *et al.* (2003) and Mahmoud and Woodall (2004), where the emphasis is on simple linear regression. Woodall *et al.* (2004) also mentioned the extension of simple linear profiles to other more complex linear profiles and listed some relevant references. Jensen *et al.* (1984) studied such a profile as well, although their model is not exactly the same. Their schemes are similar to that of Kim *et al.* (2003) but focus on controlling one parameter of the coefficients and variance individually. They propose some Shewhart-type control charts for monitoring the coefficients and variance.

The simplest case of model (1), the straight line regression model, is considered by Kang and Ablin (2000), Kim *et al.* (2003), Mahmoud and Woodall (2004) and Mahmoud *et al.* (2005). Denote by $\{(x_i, y_{ij}),\ i = 1, 2, \cdots, n\}$ the jth random sample collected over time. When the process is in control, the relationship between the response and explanatory variables is assumed to be

$$y_{ij} = A_0 + A_1 x_i + \varepsilon_{ij},\ i = 1, 2, \cdots, n, \tag{2}$$

where the ε_{ij}/σ is an i.i.d standard normal random variable.

By using the coded explanatory values, Kim *et al.* (2003) obtained the following alternative form of the underlying model

$$y_{ij} = B_0 + B_1 x_i^* + \varepsilon_{ij},\ i = 1, 2, \cdots, n, \tag{3}$$

where $B_0 = A_0 + A_1\bar{x}$, $B_1 = A_1$, $x_i^* = (x_i - \bar{x})$ and $\bar{x} = \frac{1}{n}\sum_{i=1}^{n} x_i$. For the jth sample, the least square estimators for B_0, B_1 and σ^2 are, respectively,

$$b_{0j} = \bar{y}_j, \quad b_{1j} = \frac{S_{xy(j)}}{S_{xx}}, \quad MSE_j = \frac{1}{n-2}\sum_{i=1}^{n}(y_{ij} - b_{1j}x_i^* - b_{0j})^2, \tag{4}$$

where $\bar{y}_j = \frac{1}{n}\sum_{i=1}^{n} y_{ij}$, $S_{xx} = \sum_{i=1}^{n}(x_i - \bar{x})^2$ and $S_{xy(j)} = \sum_{i=1}^{n}(x_i - \bar{x})y_{ij}$. Note that these three estimators are independent. Thus, they proposed to use three EWMA charts ($\text{EWMA}_I, \text{EWMA}_S, \text{EWMA}_E$) to detect if the Y-intercept (B_0), slope (B_1) and standard deviation (σ) had changed, respectively. They are

$$\begin{aligned}
&\text{EWMA}_I(j) = \theta b_{0j} + (1-\theta)\text{EWMA}_I(j-1) \\
&\text{EWMA}_S(j) = \theta b_{1j} + (1-\theta)\text{EWMA}_S(j-1) \\
&\text{EWMA}_E(j) = \max\Big\{\theta ln(MSE_j) + (1-\theta)\text{EWMA}_E(j-1), \ln(\sigma^2)\Big\},
\end{aligned}$$

where $\text{EWMA}_I(0) = B_0$, $\text{EWMA}_S(0) = B_1$, $\text{EWMA}_E(0) = \ln(\sigma^2)$ and θ is a smoothing constant. The three EWMA charts are used jointly, and the profile change is detected as one of the chart signals. Their ARL comparisons show that the three EWMA charts are more effective than Kang and Albin's (2000) methods in terms of detecting sustained shifts in the Y-intercept and slope, and increases in the error variance. The three EWMA charts are particularly effective in detecting shifts in the slope of the line, i.e., the changes in parameter B_1 of equation (3). Also, the authors argued that their method seemed more interpretable. Thus, in our paper, the combined multiple EWMA charts approach (denoted as KMW chart hereafter) is used as a benchmark for comparisons with our proposed scheme.

Note that monitoring simple linear profiles that have three parameters to be controlled is similar to monitoring the two parameters of mean (μ) and variability (σ^2) simultaneously in conventional SPC applications. The combination of two EWMA charts is usually required to monitor both the mean and variability. Gan (1995) suggested a simple procedure to design a combination using a two-sided EWMA chart for the mean and two one-sided EWMA charts for the variability. His method is similar to the approach by Kim *et al.* (2003). One of their difference is the number of the parameters to be controlled, and another difference is that Kim *et al.* (2003) only considered the upper-sided chart for detecting the standard deviation. Reynolds and Stoumnos (2001) considered the use of two EWMA charts as well for individual observations.

As we can see, the KMW approach requires three EWMA charts (even more, another one-sided EWMA chart may be needed to detect a decrease in variance) to be handled side by side, each one having a statistic that needs to be updated and plot-

ted for every sample. Such a scheme may be manageable for a simple linear profile case, but it can become quite complicated and infeasible for a general linear profile, as the setup of general profile charting schemes requires even more control charts to be combined simultaneously to monitor these additional parameters. Hence, the design, implementation and performance assessment of such a combined scheme will be rather complex and impractical.

In our paper, we purpose to use one single chart to monitor all the profile parameters so that the design and operation of the monitoring scheme can be greatly simplified. Here, we firstly consider the Phase II case in which the in-control (IC) values of parameters β and σ^2 are assumed to be known, i.e., it is assumed that the IC data set used in Phase I is large enough so that errors associated with estimating the three parameters can be neglected. The case of monitoring the general linear profiles with estimated parameters will be discussed in Section 9.

4 A Novel Multivariate EWMA Chart for Monitoring a General Linear Profile

In this section, we will propose a novel MEWMA scheme to monitor a general linear profile.

To monitor a general linear profile model (1), there are $p+1$ parameters, p coefficients and the standard deviations σ, to be controlled simultaneously. Following the notation in model (1), we define

$$\mathbf{Z}_j(\beta) = (\mathbf{X}^\tau\mathbf{X})^{\frac{1}{2}}(\widehat{\beta}_j - \beta)/\sigma \tag{5}$$

$$\mathbf{Z}_j(\sigma) = \Phi^{-1}\left\{F\big((n-p)\widehat{\sigma}_j/\sigma^2; n-p\big)\right\}, \tag{6}$$

where $\widehat{\beta}_j = (\mathbf{X}^\tau\mathbf{X})^{-1}\mathbf{X}^\tau\mathbf{Y}_j$, $\widehat{\sigma}_j = \frac{1}{n-p}(\mathbf{Y}_j - \mathbf{X}\widehat{\beta}_j)^\tau(\mathbf{Y}_j - \mathbf{X}\widehat{\beta}_j)$, $\Phi^{-1}(\cdot)$ is the inverse of the standard normal cumulative distribution function and $F(\cdot;\nu)$ is the chi-square distribution function with ν degrees of freedom (χ^2_ν). Note that this type of transformation with the use of an EWMA chart have been suggested by Quesenberry (1995) and Chen *et al.* (2001). Denote $\mathbf{Z}_j$ as $(\mathbf{Z}_j(\beta), \mathbf{Z}_j(\sigma))^\tau$, which is known as a $(p+1)$-variate random vector. The vector is assumed to be multivariate normally distributed with a mean zero and an identity covariance matrix when the process is

in control. Such a transformation has fairly nice properties: the distribution of this random vector is independent of the sample size, n, when the process is in control and therefore we can handle the case of variable sample size conveniently. Moreover, the choice of the control limits will not be affected by n so that the control chart can be designed more easily. Another advantage of transforming $\widehat{\sigma}_j$ to $\mathbf{Z}_j(\sigma)$ is that the distribution of $\mathbf{Z}_j(\sigma)$ would be symmetric, so that the control chart can be sensitive to decreases in the standard deviation as well.

Here, the EWMA charting statistic is defined as:

$$\mathbf{W}_j = \lambda \mathbf{Z}_j + (1-\lambda)\mathbf{W}_{j-1} \quad j = 1, 2, \cdots, \tag{7}$$

where $\mathbf{W}_0$ is a $p+1$-dimensional starting vector and λ is a parameter (chosen such that $0 < \lambda \leq 1$) that regulates the magnitude of the smoothing. The chart signals if

$$U_j = \mathbf{W}_j^{\tau} \mathbf{W}_j > L\frac{\lambda}{2-\lambda}, \tag{8}$$

where $L > 0$ is chosen to achieve a specified IC ARL. This control scheme can be deemed as a special application of MEWMA charts. The MEWMA chart was first proposed by Lowry *et al.* (1992). The design of MEWMA charts was investigated by Prabhu and Runger (1997).

In this paper, the smoothing constant, λ, in equation (7) is first taken to be 0.2 in our numerical study, which is consistent with Kim *et al.* (2003). In general, a smaller λ leads to a quicker detection of smaller shifts (Lucas and Saccucci (1990) and Prabhu and Runger (1997)). The starting vector, $\mathbf{W}_0$, is chosen to be zero and the control limits, L, are fixed according to the designed IC ARL and λ.

Through the transformation, the control limits of the proposed MEWMA chart are independent of size, n. Therefore, the control limits, L, can be conveniently tabulated as in Table 1. Here, the values of L are provided for various values of λ and IC ARL when $p = 2$ corresponds to the simple linear regression model. To determine other values of p, λ and IC ARL, a computer program is available from the authors upon request.

Table 1 The control limits L of our proposed MEWMA chart for various λ and IC ARL when $p = 2$

	λ							
ARL	0.05	0.10	0.15	0.20	0.25	0.30	0.40	0.50
200.0	9.38	10.79	11.47	11.87	12.14	12.32	12.56	12.69
370.4	11.06	12.36	12.97	13.34	13.57	13.74	13.94	14.04
500.0	11.85	13.10	13.69	14.04	14.26	14.41	14.60	14.70

In this paper, we evaluate the charting performance by ARL. Runger and Prabhu (1996) and Rigdon (1995a, 1995b) presented theoretical developments with Markov chains and integral equations, respectively, to determine the performance of MEWMA charts. Here, we extend the work of Runger and Prabhu (1996) and easily calculate the IC and OC ARL of the proposed MEWMA chart via the Markov chain model. In Kim *et al.* (2003), the performance of their KMW chart is analyzed through simulations. The control limits of the three EWMA charts are chosen so that each individual chart has the same IC ARL, while jointly achieving a specified overall IC ARL. The determination of control limits for the KMW chart by simulation is not trivial, because large numbers of simulated runs are required to obtain an acceptable standard error. Moreover, as the control limits of the KMW chart depend on the sample size, n, as well, the design of this scheme could be tedious. Although a three-dimensional Markov chain may be explored to evaluate the performance of the KMW chart, there would be considerable computing burden.

Kang and Albin (2000) proposed an alternative using the T^2 chart, which is also a single multivariate chart that monitors a profile. The T^2 chart is a Shewhart-type multivariate chart, while our proposed chart is a EWMA-type. In addition to the difference in chart type, we use a random vector with mean zero and an identity covariance matrix that contains the transformation of the standard deviation while their T^2 chart does not. The resulting advantage is that our proposed chart would be effective in detecting both the increase and decrease in the standard deviation and sensitive to small and moderate shifts as well.

Another alternative that may also be applied to the linear profile case is the Max-EWMA chart proposed by Chen *et al.* (2001). Their chart monitors the maximum absolute value of $\mathbf{W}_j$'s $p+1$ components instead of U_j. Performance comparisons of these two control schemes have been conducted (available from the authors) and numerical results show that there is no significant difference between them. However,

similar to the drawback of the KMW chart, the performance of the MaxEWMA chart is difficult to evaluate because this needs to be done through simulations. Although Calzada *et al.* (2004) use a two-dimensional integral equation to obtain the ARLs for the chart proposed by Chen *et al.* (2001), extending this method to even the three-dimensional case would require excessive computing load.

Note that Kim *et al.* (2003) and Woodall *et al.* (2004) mention that the multivariate EWMA chart may be used to improve the performce of the T^2 chart but the interpretation of an out-of-control signal would not be straightforward. However, in Section 8, we provide a simple diagnostic aid that can provide information for identifying and isolating the out-of-control signal with at least comparable diagnostic performance to that of the KMW scheme.

5 Adding Variable Sampling Features to the Proposed Profile Monitoring Scheme

The variable sampling interval (VSI) scheme is a known approach to enhancing the efficiency of SPC monitoring schemes. However, existing multiple chart profile monitoring schemes such as the KMW scheme cannot easily incorporate the VSI feature. Because MEWMA is a single chart, a VSI version can be designed and implemented for a general linear profile without much modification and can largely improve the efficiency in detecting profile changes.

The conventional practice in applying SPC control charts to monitoring a process is to use a fixed sampling rate (FSR) that takes samples of fixed sample size (FSS) with a fixed sampling interval (FSI). In recent years, several modifications have been suggested to improve traditional FSR policies that provide better performance than conventional charts in the sense of quicker responses to a process change. Among them, adopting a variable sampling interval in a control chart instead of a FSI is one of the most popular and useful approaches to improving the detection ability. In a VSI control chart, the sampling interval is varied as a function of the control statistic. The basic idea of the VSI feature is to use a shorter sampling interval if there is some indication of a possible change, but to use a longer sampling interval if there is no such indication.

Many researchers have contributed to the theory and practice of the VSI chart. Most work on developing VSI control charts focuses on monitoring the mean, such as Reynolds *et al.* (1988), Reynolds and Arnold (1989), Reynolds (1989), Reynolds *et al.* (1990), Runger and Montgomery (1993) and Reynolds and Arnold (2001), *etc.* Chengular *et al.* (1989) introduced a VSI Shewhart chart for monitoring the mean and variance with a sample size of $n > 1$. Reynolds and Stoumbos (2001) added the VSI feature to various combinations of control charts to detect the shift in the mean and variance using individual observations. There are rather few research works on VSI multivariate control charts. Aparisi and Haro (2001) considered a VSI control chart based on Hotelling's statistic. Reynolds and Kim (2005a, 2005b) recently investigated MEWMA control charts based on sequential sampling and unequal sample sizes respectively.

Past work on VSI control charts (see e.g. Reynolds (1989)) has shown that it is sufficient to use only two possible values for the sampling intervals. Hence, in this paper, we consider two possible interval values, say $0 < d_1 \leq d_2$. To apply the VSI feature to the MEWMA control chart, additional warning limits $0 \leq L_1 \leq L$ inside the control limits are applied to determine which sampling interval to use next. In particular, a long sampling interval, d_2, should be used after the sample, j, is obtained, if U_j falls inside the warning limits of $L_1\frac{\lambda}{2-\lambda}$. On the other hand, a short sampling interval, d_1, should be used if U_j falls outside of these limits but inside the control limits of $L\frac{\lambda}{2-\lambda}$. If U_j falls outside of the control limits, then an out-of-control signal would be triggered as in the case of the traditional FSI MEWMA chart.

When evaluating the statistical performance of a VSI control chart, both the average time to signal (ATS) and average number of samples to signal (ANSS) should be considered, because the ATS is not simply a constant multiple of the ANSS, as is the case with an FSI chart. In the comparative study in this paper, we require that all of the charts being compared have the same in-control sampling rate and the same false alarm rate. This ensures that the charts being compared will have the same ATS and ANSS when the process is in control. When different control charts being compared are designed to have the same IC ATS and ANSS, these charts can then be fairly compared according to the steady-state ATS (SSATS). The SSATS is defined as the expected time from the point of the shift to the point at

which the chart signals, under the assumption that the control statistic has reached a stationary or steady state distribution by the time the shift occurs.

Discussion of the assumptions used in defining the SSATS can be found in Reynolds *et al.* (1990). The computation of SSATS is more complicated than that of ATS for the reason that the point at which the shift occurs may fall within the interval between two samples. For the VSI and FSI MEWMA charts, the ATS and SSATS can also be evaluated by the Markov chain approximation, which is detailed in Section 6. The performance comparisons between FSI and VSI schemes are presented in Section 7.

Here, Table 2 provides the values of the warning limits, L_1, that will make the in-control ATS and ANSS equal to the ATS and ANSS with the corresponding control limits, L, tabulated in Table 1.

Table 2 The warning limits L_1 of our proposed MEWMA chart for various λ and IC ATS when $p = 2$

$(d_1, d_2) = (0.1, 1.9)$								
	λ							
ATS	0.05	0.10	0.15	0.20	0.25	0.30	0.40	0.50
200.0	2.038	2.190	2.247	2.278	2.297	2.310	2.326	2.334
370.4	2.172	2.265	2.299	2.317	2.327	2.335	2.344	2.349
500.0	2.217	2.290	2.315	2.328	2.337	2.342	2.350	2.354
$(d_1, d_2) = (0.5, 1.25)$								
	λ							
ATS	0.05	0.10	0.15	0.20	0.25	0.30	0.40	0.50
200.0	2.925	3.142	3.225	3.268	3.296	3.316	3.339	3.349
370.4	3.120	3.254	3.301	3.329	3.345	3.356	3.369	3.375
500.0	3.186	3.290	3.329	3.347	3.358	3.367	3.378	3.383
$(d_1, d_2) = (0.25, 1.50)$								
	λ							
ATS	0.05	0.10	0.15	0.20	0.25	0.30	0.40	0.50
200.0	2.536	2.723	2.795	2.832	2.855	2.872	2.892	2.903
370.4	2.704	2.818	2.860	2.881	2.896	2.905	2.917	2.923
500.0	2.760	2.849	2.882	2.899	2.909	2.916	2.924	2.928

6 ARL and ATS Calibrations of the Proposed Profile Monitoring Scheme

Because our proposed chart is a special case of the MEWMA chart proposed by Lowry *et al.* (1992), the Markov chain approximation presented by Runger and Prabhu (1996) may be extended to calculate our ARLs. Here, we only briefly describe the Markov chain approximation method, but highlight some necessary modifications. For more detail on the Markov chain approximation for a conventional MEWMA chart, readers may refer to Runger and Prabhu (1996).

First, because the vector, $\mathbf{Z}$, (here we suppress the sample number j for simplicity) is a vector with a mean zero and identity covariance. The IC ARL can be evaluated by the same approach as in Runger and Prabhu (1996). A one-dimensional Markov chain is used to approximate the IC ARL. Define the $(m+1)$ by $(m+1)$ transition probability matrix, $\mathbf{P} = (p_{ij})$, where the element p_{ij} denotes the probability of a transition from state i to j, and $(m+1)$ is the number of transition states. Now, we have for $i = 0, 1, 2, \cdots, m$,

$$p_{ij} = f_1^{-1}\big((j+0.5)^2 g^2/\lambda^2; p+1; \xi\big) - f^{-1}\big((j-0.5)^2 g^2/\lambda^2; p+1; \xi\big) \quad 0 < j \leq m$$
$$p_{i0} = f_1^{-1}\big((0.5)^2 g^2/\lambda^2; p+1; \xi\big) \quad j = 0$$

where $g = (L\frac{\lambda}{2-\lambda})^{\frac{1}{2}}/(m+1)$, $\xi = [(1-\lambda)ig/\lambda]^2$ and $f_1^{-1}(\cdot; \nu; \xi)$ is the inverse function of the noncentral chi-squared distribution function with ν degrees of freedom and non-centrality parameter ξ. The IC ARL can then be evaluated by

$$\text{ARL} = \mathbf{l}^\tau (\mathbf{I} - \mathbf{P})^{-\mathbf{1}} \mathbf{1},$$

where $\mathbf{I}$ denotes the $(m+1)$-dimensional identity matrix and $\mathbf{l}$ is a $(m+1)$ vector with a 1 as the first element. Note that a computer program calculates the ARL of the MEWMA chart presented by Molnau *et al.* (2001) can be directly utilized.

Next, we consider the approximation under an out-of-control condition. Lowry *et al.* (1992) and Runger and Prabhu (1996) have shown that the off-target performance of the MEWMA chart may be determined by assuming, without loss of generality, that the off-target mean vector is $\delta\mathbf{l}$. The two-dimensional Markov chain can then be used to analyze the OC ARL of MEWMA. One dimension that includes

$m_2 + 1$ states is used to analyze the properties of IC components, while the other dimension of the Markov chain that has $2m_1+1$ transition states is for analyzing the performance of the OC component. Therefore, a $(2m_1 + 1) \times (m_2 + 1)$ dimensional matrix is utilized.

In our case, when the regression coefficients of a linear profile change, i.e., from β to β^*, the noncentrality parameter, δ, is

$$\delta = \frac{1}{\sigma}\sqrt{(\beta^* - \beta)^\tau(\mathbf{X}^\tau\mathbf{X})(\beta^* - \beta)}. \tag{9}$$

However, when the standard deviation of the profile changes from σ to $\delta\sigma$, both the distributions of $\mathbf{Z}(\beta)$ and $\mathbf{Z}(\sigma)$ would also change, although their independency still holds. Furthermore, the $\mathbf{Z}(\sigma)$ would be no longer normally distributed. Thus, some modifications are necessary to obtain the OC ARL in the profile case.

In fact, if we divide $\mathbf{Z}$ by δ, the distributions of $\mathbf{Z}(\beta)$ would be a p-dimensional vector that was standard multivariate normally distributed. It can be verified that the run-length distributions of the EWMA of $\mathbf{Z}/\delta$ with the control limit $L\frac{\lambda}{2-\lambda}/\delta$ turn out to be the same as that of the EWMA of $\mathbf{Z}$ with the control limit $L\frac{\lambda}{2-\lambda}$. Hence, a two-dimensional Markov chain can still be used for this case. The on target one-dimensional Markov chain can then be obtained by a similar approach as the IC case described above with the control limits $L\frac{\lambda}{2-\lambda}/\delta$ replacing $L\frac{\lambda}{2-\lambda}$, and degrees of freedom $p + 1$ replacing p in the f_1^{-1} function. Also, the transitional probability of the off-target part, $\mathbf{Z}(\sigma)/\delta$, from state i to j denoted by $v(i, j)$ can be obtained as follows: similar to Runger and Prabhu (1996), we partition the control limits, $-L\frac{\lambda}{2-\lambda}/\delta$ and $L\frac{\lambda}{2-\lambda}/\delta$, into $2m+1$ states of length g. Let $c_i = -L\frac{\lambda}{2-\lambda}/\delta+(i-0.5)g$. Then,

$$\begin{aligned}
v(i,j) = Pr\Big\{&\frac{1}{\lambda}\big[-L\frac{\lambda}{2-\lambda}/\delta + (j-1)g - (1-\lambda)c_i\big] < \mathbf{Z}(\sigma)/\delta \\
&< \frac{1}{\lambda}\big[-L\frac{\lambda}{2-\lambda}/\delta + jg - (1-\lambda)c_i\big]\Big\} \\
= F\Big(&F^{-1}\Big(\Phi\Big(\frac{\delta}{\lambda}\big[-L\frac{\lambda}{2-\lambda}/\delta + jg - (1-\lambda)c_i\big]\Big); n-2\Big)/\delta^2; n-2\Big) \\
-F\Big(&F^{-1}\Big(\Phi\Big(\frac{\delta}{\lambda}\big[-L\frac{\lambda}{2-\lambda}/\delta + (j-1)g - (1-\lambda)c_i\big]\Big); n-2\Big)/\delta^2; n-2\Big),
\end{aligned}$$

where F is the chi-squared distribution function defined in Section 3. After that, we combine the two one-dimensional transition probability matrices into a bivariate

Markov chain by the methodology of Runger and Prabhu (1996). The OC ARL when a shift in the standard deviation occurs can then be obtained.

Now, we consider the calculation of the ATS and SSATS for profile monitoring. When the process is in control, we can obtain a one-dimensional transition probability matrix, $\mathbf{P}$, from the calculation of the ARL for the MEWMA chart. By using the same methodology as in Reynolds *et al.* (1990), the IC ATS can be expressed as

$$\text{ATS} = d_0 + \mathbf{l}^\tau(\mathbf{I} - \mathbf{P})^{-\mathbf{1}}\mathbf{d},$$

where d_0 is the interval between the beginning of the process and the time the first sample is taken, and $\mathbf{d}$ is a $(m+1)$ vector. The ith element of $\mathbf{d}$ corresponds to the interval to be taken after the control statistics fall inside the state, i. The approach to determine the $\mathbf{d}$ is as follows: when the upper limit of ith state is smaller than the warning limit, say $(i+0.5)g \leq (L_1\frac{\lambda}{2-\lambda})^{\frac{1}{2}}$, then the ith element of $\mathbf{d}$ is d_2. When the lower limit of the ith state is larger than the warning limit, say $(i-0.5)g > (L_1\frac{\lambda}{2-\lambda})^{\frac{1}{2}}$, then the ith element of $\mathbf{d}$ is d_1. When the warning limit falls between the the upper limit and lower limit, the extrapolations are used. In this paper, all of the numerical results are for the general case with $d_0 = 1$.

To compute the SSATS, the bivariate Markov chain illustrated above can be applied as well. Note that although the two-dimensional Markov chain is used to determine the statistical properties of the MEWMA chart when the process is out of control, it is also be valid in the in-control case. Define $\mathbf{Q}_0$ as the $(2m_1+1)\times(m_2+1)$-dimensional transition probability matrix when the process is in control. Let $\mathbf{d}$ be a $(2m_1+1)\times(m_2+1)$ vector, and the ith element of this vector corresponds to the interval being taken after the control statistics fall inside the state, i. Denote π to be the normalized eigenvector subject to $\pi^\tau\mathbf{Q_0} = \pi^\tau$. Suppose α is the vector of starting probabilities that the shift occurs in an interval between samples. Then, α^τ can be expressed in matrix notation, $\alpha = \frac{\pi^\tau\mathbf{D}}{\pi\mathbf{L}}$, where $\mathbf{D}$ is a diagonal matrix with $\mathbf{d}$ on the diagonal. Then, the SSATS can be expressed as

$$\text{SSATS} = \alpha^\tau[(\mathbf{I} - \mathbf{Q})^{-\mathbf{1}} - \frac{\mathbf{1}}{\mathbf{2}}\mathbf{I}]\mathbf{d},$$

where $\mathbf{Q}$ is a $(2m_1+1)\times(m_2+1)$ dimension matrix when the process is out of control. The $\mathbf{Q}$ can then be calculated by the same method used to calculate the OC ARLs.

In addition, similar to Runger and Prabhu (1996), we compute $(\mathbf{I}-\mathbf{P})\mathbf{b}=\mathbf{1}$, which can be quicker than computing $(\mathbf{I}-\mathbf{P})^{-\mathbf{1}}\mathbf{1}$, in obtaining the ARL and ATS.

In this paper, the IC ARL and ATS are obtained using $m = 100$ and the OC ARL and SSATS are obtained using $m_1 = m_2 = 30$.

We have conducted simulations to verify the accuracy of the Markov chain approximation for the profile monitoring case, and the results are very satisfactory.

7 Monitoring Performance Comparisons

In this section, we investigate the monitoring performance of the proposed MEWMA scheme via ARL comparisons. Although our proposed control chart can be used to monitor the general linear profile model (1), there seem to be no other effective and comparable methods for such a model except for the simple straight line model (2), i.e., $p = 2$ in model (1). Hence, we compare the performance of our proposed control chart and the KMW chart under model (2) (or (3) equivalently).

For simplicity and consistency with the literature, the change-point is assumed to be $\tau = 0$, and only the case of overall IC ARL=200 is considered. The underlying IC model is the same as that in Kang and Albin (2000), in which the parameters in the in-control model are $A_0 = 3$, $A_1 = 2$ and $\sigma^2 = 1$, $x_i = 2, 4, 6, 8$. In Kim *et al.* (2003), the control limits are set to be 3.0156, 3.0109 and 1.3723 for the three EWMA charts ($\text{EWMA}_I, \text{EWMA}_S, \text{EWMA}_E$), respectively, when the smoothing constant, λ, is chosen to be 0.2. In the case of known parameters, this design has an overall IC ARL of roughly 200 and the IC ARL of each chart is about 584. The ARL results of the KMW and MEWMA charts are evaluated with 50,000 simulations and Markov chain approximation, respectively. Moreover, the types of shifts considered in this paper are consistent with those in Kim *et al.* (2003).

We compared our proposed MEWMA chart with the KMW chart in terms of out-of-control ARL. The OC ARLs of our MEWMA chart and that of the KMW chart for detecting shifts in A_0, A_1, σ and B_1 are given in Table 3. Note that when the process parameter A_1 is changed to $A_1 + \delta_1\sigma$, it can be easily checked that the noncentrality parameter, δ, in (9) becomes $\delta_1\sqrt{n \cdot \bar{X} + S_{xx}}$. From this table, we observe that for a detection of shift in A_1, the two charts have very similar performances with large

shifts. With small and moderate shifts, our proposed MEWMA performs a little better than the KMW chart. Also, for detecting a shift in the standard deviation, our proposed MEWMA chart performs better than the KMW chart, except with a very small shift. Our proposed MEWMA chart has a slight disadvantage in detecting the moderate and large shifts in intercept A_0 and B_1 compared with the KMW chart, but the difference between them seems negligible.

Table 3 ARL comparisons between MEWMA and KMW charts for shifts in A_0, A_1, the standard deviation and B_1.

A_0			A_1		
δ_1	MEWMA	KMW	δ_1	MEWMA	KMW
0.1000	131.5	133.7	0.0250	99.0	101.6
0.2000	59.9	59.1	0.0375	57.4	61.0
0.3000	29.6	28.3	0.0500	35.0	36.5
0.4000	17.2	16.2	0.0625	23.1	24.6
0.5000	11.5	10.7	0.0750	16.4	17.0
0.6000	8.5	7.9	0.1000	9.8	10.3
0.8000	5.8	5.1	0.1250	6.9	7.2
1.0000	4.1	3.8	0.1500	5.3	5.5
1.5000	2.6	2.4	0.2000	3.7	3.8
2.0000	2.0	1.9	0.2500	2.9	2.9
σ			B_1		
δ_1	MEWMA	KMW	δ_1	MEWMA	KMW
1.1000	76.2	72.8	0.0500	120.5	120.8
1.1500	48.7	48.1	0.0750	77.3	77.3
1.2000	33.2	33.5	0.1000	50.0	49.1
1.2500	24.1	24.9	0.1500	24.0	22.8
1.3000	18.4	19.4	0.2000	14.0	13.1
1.4000	12.1	12.7	0.2500	9.5	8.9
1.6000	7.0.	7.2	0.3000	7.1	6.6
1.8000	4.9	5.1	0.4000	4.7	4.4
2.2000	3.1	3.2	0.5000	3.6	3.3
2.6000	2.3	2.5	0.7000	2.5	2.3
3.0000	1.9	2.1	0.9000	2.0	1.9

Note that in detecting the change of standard deviation, the KMW chart is an upper-sided scheme, i.e., it is for detecting an increase but not directly for a decrease in variance. However, our approach can detect the decreases in variance without modification. The ARL results are shown in Table 4.

Table 4 ARLs of the MEWMA chart in detecting a decrease in variance.

δ_1	0.10	0.15	0.20	0.25	0.30	0.35	0.40
ARL	3.3	3.9	4.5	5.3	6.4	7.8	9.7
δ_1	0.45	0.50	0.55	0.60	0.65	0.70	0.75
ARL	12.5	16.5	22.9	33.0	49.1	74.9	114.5

Simultaneous shifts in the intercept and slope in model (3) are also considered in this paper. The OC ARL values are obtained and summarized in Table 5. The magnitudes of shifts in intercept (B_0) δ_1 and slope (B_1) δ_2 are consistent with Kim *et al.* (2003). It can be clearly seen that the noncentrality parameter is $\delta = \sqrt{\delta_1^2 n + \delta_2^2 S_{xx}}$. Here, the MEWMA chart performs better than the KMW chart in most cases except when one of δ_1 and δ_2 is very large but the other is very small.

Table 5 The ARL comparisons between MEWMA and KMW charts under combinations of intercept (δ_1) and slope (δ_2) shifts in model (3)

MEWMA		δ_2									
KMW		0.025	0.050	0.075	0.100	0.125	0.150	0.175	0.200	0.225	0.250
	0.05	155.8	111.0	72.9	48.0	32.8	23.5	17.7	13.9	11.3	9.5
		157.6	114.7	74.8	48.3	32.2	22.5	16.9	13.2	10.7	8.9
	0.10	118.0	89.2	62.1	42.8	30.2	22.2	16.9	13.5	11.0	9.3
		122.1	94.6	66.4	44.9	30.7	21.9	16.6	13.1	10.6	8.9
	0.15	82.2	66.3	49.5	36.1	26.7	20.2	15.8	12.8	10.6	9.0
		84.6	70.8	54.5	39.6	28.5	20.9	16.1	12.8	10.4	8.8
	0.20	56.4	48.0	38.2	29.6	22.9	18.1	14.5	12.0	10.1	8.7
		57.1	51.1	42.4	33.3	25.4	19.5	15.4	12.4	10.2	8.7
δ_1	0.25	39.5	35.0	29.4	24.0	19.5	15.9	13.2	11.1	9.5	8.2
		39.5	36.5	32.3	27.1	22.0	17.8	14.4	11.9	10.0	8.5
	0.30	28.7	26.2	22.9	19.6	16.5	13.9	11.8	10.2	8.8	7.8
		28.2	26.9	24.7	22.0	18.8	15.7	13.2	11.2	9.6	8.3
	0.35	21.7	20.2	18.3	16.1	14.0	12.2	10.6	9.3	8.2	7.3
		20.9	20.2	19.1	17.6	15.8	13.9	12.1	10.5	9.1	8.0
	0.40	17.0	16.1	14.9	13.5	12.0	10.7	9.5	8.5	7.6	6.9
		16.2	15.9	15.3	14.5	13.5	12.1	10.9	9.7	8.6	7.6
	0.45	13.7	13.2	12.4	11.4	10.5	9.5	8.6	7.8	7.1	6.5
		13.1	12.9	12.6	12.1	11.4	10.6	9.8	8.9	8.0	7.3
	0.50	11.4	11.1	10.5	9.9	9.2	8.5	7.8	7.2	6.6	6.1
		10.8	10.8	10.6	10.3	9.9	9.3	8.7	8.1	7.5	6.9

We may conclude from Tables 3-5 that for detecting shifts in simple linear profiles, the single scheme MEWMA chart has at least comparable performance with the combination scheme KMW chart. The MEWMA chart usually outperforms the

KMW chart when several parameters have changed. Some other numerical results have been obtained (available from the authors) for shifts in combinations of either B_0 and σ or B_1 and σ to validate this argument.

Finally, we show the improved performance gained in terms of ATS by adding the VSI feature to the MEWMA chart for monitoring linear profiles. Although the VSI feature may also be applied to the KMW chart, the design of the combination of three VSI EMWA charts is not at all trivial because three warning limits and three control limits need to be simultaneously chosen so that all charts have the same individual IC average sampling rate and IC average false-alarm rate. Here, we compare only the SSATS of the FSI and VSI MEWMA charts. We do not tabulate the SSATS of the FSI KMW chart because the performance of the KMW chart would be similar to that of the MEWMA chart. Table 6 presents the SSATS values of the VSI and FSI MEWMA charts for the linear profiles models (2). The shifts in intercept and standard deviation are investigated. The IC ATS and ANSS of each chart are both set to be equal to 200.0. That is, the average IC sampling rate of the VSI chart is one sample per unit time. All the numerical results listed in Table 6 are obtained by Markov chain approximation.

Table 6 SSATS comparisons between FSI MEMWA and VSI MEWMA charts for the shift in intercept and standard deviation.

A_0					σ				
δ_1	FSI	VSI			δ_1	FSI	VSI		
		d_1=0.5 d_2=1.25	$d_1 = 0.25$ $d_2 = 1.5$	$d_1 = 0.1$ $d_2 = 1.9$			d_1=0.5 d_2=1.25	$d_1 = 0.25$ $d_2 = 1.5$	$d_1 = 0.1$ $d_2 = 1.9$
0.1	127.9	124.4	122.2	120.0	0.1	2.7	2.1	1.9	1.8
0.2	57.6	51.9	48.3	45.2	0.3	5.8	4.3	3.6	3.3
0.4	28.1	23.3	20.4	18.1	0.5	15.9	11.2	8.7	7.1
0.4	16.1	12.6	10.6	9.2	0.7	73.8	63.9	57.6	51.1
0.5	10.6	8.0	6.6	5.8	1.1	73.2	68.9	66.3	63.9
0.6	7.6	5.7	4.8	4.2	1.2	31.2	27.4	25.2	23.4
0.8	4.8	3.6	3.1	2.8	1.4	16.9	14.1	12.5	11.4
1.0	3.4	2.6	2.3	2.1	1.8	10.8	8.8	7.7	6.9
1.5	2.0	1.6	1.4	1.4	2.2	4.0	3.2	2.7	2.6
2.0	1.4	1.1	1.0	1.1	2.6	2.4	1.9	1.7	1.7
3.0	0.8	0.7	0.8	0.9	3.0	1.3	1.1	1.1	1.2

From Table 6, we conclude that adding the VSI feature can provide quite sub-

stantial reductions in the time required to detect small and moderate shifts. The results presented here are fairly consistent with previous research on univariate VSI control charts. In general, the interval, d_1, should be as small as possible for better statistical performance (Reynolds *et al.* (1990)), so it usually depends on how soon it is feasible to sample again after the current sample is taken. The sampling interval, d_2, on the other hand, could be chosen to be long so that the resulting control chart will have an acceptable average sampling rate. Similar conclusions can be obtained for other types of changes as well.

8 Diagnostic Aids in Profile Monitoring

In the practice of quality control, in addition to detecting a process change quickly, it is also critical to diagnose the change and to identify which parameter or parameters in a profile have shifted after an out-of-control signal occurs. Such diagnosis is particularly important in general profile monitoring, where there are more process parameters involved. A diagnostic aid to locate the change point in the process and to isolate the type of parameter change in a profile will help an engineer to identify and eliminate the root cause of a problem quickly and easily. In this section, we discuss the diagnosis of a general linear profile and provide a systematic diagnostic approach to identify the location of the change and which parameters in the profile have changed.

8.1 Estimate of the Change Point in Profile Monitoring

To identify the location of a change point in profile monitoring, a maximum likelihood estimator of the change-point statistic is used. We assume that an out-of-control signal is triggered at subgroup k by the MEWMA chart. Our suggested estimator of the change-point, τ, of a step shift is given by

$$\widehat{\tau} = \underset{0 \le t < k}{arg\ \max}\{lr(tn, kn)\}, \tag{10}$$

where $lr(tn, kn)$ is the generalized likelihood ratio statistic. The expressions of $lr(tn, kn)$ and the involved deductions are given in Appendix. This estimator has been used for off-line non-sequential change-point detection in linear models in the

literature (see Chapter 3 of Csorgo and Horvath (1997) for more details). In this paper, we utilize it in an on-line SPC application. Zou *et al.* (2006) recently suggested a similar estimator, using a standardized generalized likelihood ratio statistic instead, when the true parameters of the linear profile are unknown. It should be noted that Nishina (1992) proposed an estimator for the process change point when a traditional EWMA control chart sends out a signal. Pignatiello and Samuel (2001) showed that the MLE method performs much better than the method proposed by Nishina (1992) for a conventional process change. We think that this result should be valid for the linear profile model as well, so we do not investigate Nishina's (1992) method further in this paper.

Here, we conduct simulations to evaluate the effectiveness of the estimator (10). In the simulations, the change-point $\tau = 100$ is used. Fifty thousand independent series are generated in the simulations. Note that any series in which a signal occurs before the $\tau + 1$ product observations is discarded. In Table 7, we tabulate the average (AVE) and standard deviation (SD) of the estimate $\widehat{\tau}$ for the shift in intercept and variance under model (3). Also, the observed frequencies with which the estimator are within a given number of samples around the actual τ, i.e., the probabilities $Pr(\widehat{\tau} = \tau)$, $Pr(|\widehat{\tau} - \tau| \leq 1)$, $Pr(|\widehat{\tau} - \tau| \leq 3)$ and $Pr(|\widehat{\tau} - \tau| \leq 5)$ (denoted by P_0, P_1, P_3 and P_5 in Table 7, respectively) are presented. These probabilities may provide certain indications of the precision of the estimator.

Table 7 shows that the proposed estimator performs well from the viewpoint of the average for any shift size. We can also see that $\widehat{\tau}$ has better precision as the magnitude of the shift increases. These findings about the MLE estimator for profile monitoring are consistent with Pignatiello and Samuel's (2001) conclusion about conventional non-profile monitoring.

Table 7 The average, standard deviation and precision of change point estimates for the proposed method

			B_0							σ			
δ_1	AVE	SD	P_0	P_1	P_3	P_5	δ_1	AVE	SD	P_0	P_1	P_3	P_5
0.4	102.6	13.3	0.13	0.27	0.45	0.58	1.4	100.5	10.5	0.20	0.39	0.60	0.73
0.8	99.6	7.0	0.40	0.63	0.83	0.91	1.8	99.6	6.2	0.45	0.69	0.87	0.93
1.2	99.6	4.7	0.63	0.83	0.94	0.97	2.2	99.6	4.9	0.61	0.83	0.94	0.97
1.6	99.8	2.6	0.79	0.94	0.98	0.99	2.6	99.7	3.5	0.72	0.90	0.97	0.98
2.0	99.8	2.3	0.89	0.97	0.98	0.99	3.0	99.8	2.6	0.79	0.94	0.98	0.99

8.2 Identification of the Out-of-Control Profile Parameters

After locating the change point in a profile, it is also critical to identify the specific parameter in the profile that has changed. In Kim *et al.* (2003), since their proposed chart is the combination of three EWMA charts and each chart detects the corresponding parameter, the diagnosis of any process change is easier than that of omnibus methods of Kang and Albin (2000). However, there is also a drawback in using the combination of charts to determine which parameter has changed. When one of the charts has signaled, engineers usually will only go after that specific charting parameter and ignore the possibility that there may be other parameters that have changed as well. In addition, using combination schemes such as the KMW chart to diagnose a special cause may not be appropriate for a general linear profile because the components of $\widehat{\beta}$ are usually correlated except in a simple linear profile.

At first glance, our proposed method based on a single chart seems not to be able to diagnose which parameter has changed. However, as Reynolds and Stoumbos (2005) pointed out, the control charts used as diagnostic aids do not necessarily have to be the same control charts used to determine when to signal. Similar arguments can also been found in Hawkins and Zamba (2005), where two parametric tests are used to determine if the shift comes from the mean or the variance. Thus, in this paper, we propose using a parametric test method as an auxiliary tool to determine which parameters in a profile have changed after the chart has triggered a signal. Denote

$$\tilde{\beta}_{t,k} = \frac{1}{(k-t)}(\mathbf{X}^\tau\mathbf{X})^{-1}\mathbf{X}^\tau \sum_{j=t+1}^{k} \mathbf{Y}_j \tag{11}$$

$$\tilde{\sigma}^2_{t,k} = \frac{1}{(k-t)n-p} \sum_{j=t+1}^{k} (\mathbf{Y}_j - \mathbf{X}\tilde{\beta}_{t,k})^\tau(\mathbf{Y}_j - \mathbf{X}\tilde{\beta}_{t,k}). \tag{12}$$

Assume that the MEWMA chart signaled at kth sample, after obtaining the change-point estimator $\widehat{\tau}$ using (10). The tests for the Y-intercept, standard deviation, and regression coefficients are given as follows: we use the t-test for a Y-intercept change using $(k-\widehat{\tau})n-p$ degrees of freedom and the test statistic

$$T_{test} = \frac{\sqrt{(k-\widehat{\tau})n}(\tilde{\beta}^{(1)}_{\widehat{\tau},k} - \beta^{(1)})}{\tilde{\sigma}_{\widehat{\tau},k}}, \tag{13}$$

where $\tilde{\beta}^{(1)}_{\widehat{\tau},k}$ denotes the first component of the p-dimensional vector, $\tilde{\beta}_{\widehat{\tau},k}$. Also, the χ^2-test is used for a standard deviation change using $(k-\widehat{\tau})n-p$ degrees of freedom and the test statistic

$$\chi^2_{test} = \frac{[(k-\widehat{\tau})n-p]\tilde{\sigma}^2_{\widehat{\tau},k}}{\sigma^2}. \tag{14}$$

For the rest of the $p-1$ profile parameters $(\beta^{(2)}, \cdots, \beta^{(p)})$, by considering the correlations between their estimators, we follow the work of Jensen *et al.* (1984) and use the following test with a reject region:

$$F^{(i)}_{test} : (k-\widehat{\tau})\Big(\tilde{\beta}^{(i)}_{\widehat{\tau},k} - \beta^{(i)}\Big)^2 / m_{ii}\tilde{\sigma}^2_{\widehat{\tau},k} > F_\alpha(p-1, (k-\widehat{\tau})n-p, \mathbf{R}) \tag{15}$$

for each $i = 2, \cdots, p$, where m_{ii}s are diagonal elements of $\mathbf{M} = (\mathbf{X}^\tau\mathbf{X})^{-1}$, $\mathbf{R} = diag\{m_{11}^{-\frac{1}{2}}, \cdots, m_{pp}^{-\frac{1}{2}}\}\mathbf{M}diag\{m_{11}^{-\frac{1}{2}}, \cdots, m_{pp}^{-\frac{1}{2}}\}$, is the correlation matrix for $\widehat{\beta}$, and $F_\alpha(p-1, (k-\widehat{\tau})n-p, \mathbf{R})$ is the upper α percentile of the multivariate F distribution with parameters $(p-1, (k-\widehat{\tau})n-p, \mathbf{R})$ (see Kotz, Balakrishnan and Johnson (2000)).

Here, we compare the diagnostic ability of indicating out-of-control parameters between the above hypothesis test method with $\alpha = 0.05$ and the KMW chart under a simple linear model (3). The simulation results are tabulated in Table 8.

In this table, these three digits in the first row present various combinations of parameter changes in the Y-intercept, slope and standard deviation. For example, the three digits in "100" correspond to the Y-intercept, slope and standard deviation, respectively, in which the first digit "1" means a change in the Y-intercept while the second and third digits "00" means no shift in the other two parameters. The simulated estimates of the probabilities of events occurring at "100", "010", etc for various shift patterns are presented, where the upper and lower entries are obtained by the KMW chart and the parametric tests. These probabilities indicate the accuracies of the diagnosis approaches, with the larger value indicating a higher diagnostic accuracy.

From Table 8, we may observe that for a single shift in the standard deviation, our proposed parametric test method is more effective, but for a single shift in the intercept or slope, the KMW chart actually performs better than our method. However, our proposed approach has much better performance than the KMW chart in identifying the special cause when there are simultaneous shifts in the intercept

and slope, no matter what the shift sizes are. In summary, using the hypothesis test method may alleviate the problem of the KMW chart in identifying multiple parameter changes, but at the expense of the accuracy to some extent when indeed only a single parameter (either Y-intercept or the slope) has shifted.

Table 8 A comparisons of diagnostic abilities of the method using KMW chart and parametric test for shift in B_0,B_1 and standard deviation in model (3)

δ_I	δ_S	δ_σ	100	010	001	110	101	011	111
0.4	0.0	1.0	0.942	0.029	0.027	0.001	0.002	0.000	0.001
			0.652	0.024	0.020	0.136	0.081	0.005	0.062
0.8	0.00	1.0	0.979	0.011	0.008	0.002	0.001	0.000	0.000
			0.746	0.008	0.013	0.105	0.069	0.001	0.039
0.0	0.10	1.0	0.079	0.839	0.079	0.001	0.001	0.001	0.001
			0.045	0.559	0.032	0.151	0.014	0.092	0.084
0.0	0.15	1.0	0.037	0.928	0.033	0.001	0.001	0.002	0.000
			0.026	0.631	0.021	0.134	0.008	0.090	0.068
0.0	0.0	0.1	–	–	–	–	–	–	–
			0.002	0.001	0.879	0.001	0.049	0.053	0.015
0.0	0.0	0.4	–	–	–	–	–	–	–
			0.002	0.001	0.811	0.001	0.077	0.075	0.031
0.0	0.0	1.6	0.154	0.149	0.653	0.005	0.018	0.020	0.000
			0.057	0.062	0.720	0.030	0.046	0.046	0.005
0.0	0.0	2.8	0.138	0.145	0.522	0.020	0.079	0.083	0.013
			0.033	0.032	0.810	0.021	0.026	0.029	0.003
0.2	0.1	1.0	0.408	0.532	0.050	0.009	0.001	0.001	0.000
			0.162	0.219	0.026	0.395	0.034	0.040	0.100
0.4	0.15	1.0	0.589	0.365	0.019	0.026	0.001	0.000	0.000
			0.255	0.144	0.020	0.421	0.030	0.019	0.087
0.6	0.15	1.0	0.812	0.149	0.011	0.027	0.001	0.000	0.000
			0.415	0.061	0.016	0.366	0.045	0.007	0.068
0.8	0.20	1.0	0.817	0.123	0.007	0.051	0.001	0.000	0.000
			0.412	0.044	0.016	0.405	0.035	0.004	0.060

9 Constructing the Proposed Chart when the Parameters are Estimated

So far, we have assumed that the profile parameters of the process are known in Phase II. However, in the early stages of process improvement, the process parameters, the intercept, slope and standard deviation may not be known exactly, as they are usually just estimated by m IC trial samples of size n.

Some authors have recommended using 20 to 30 samples of size 4 or 5 to estimate the process parameters for the traditional control charts (see Montgomery (2004)). Also, several authors have investigated the effect of the estimated parameters on the

performance of traditional control charts, such as Quesenberry (1993), Jones, Champ and Rigdon (2001, 2004), *etc.* They all indicated that when the number of reference samples is small, the control charts with estimated parameters may produce rather large bias in the IC ARL from the nominal value and reduce the sensitivity of the chart in detecting process changes. To attain a similar performance as the chart with known parameters, 20 or 30 historical samples seem too small. For example, for the traditional EWMA chart with $\lambda = 0.2$, 300 samples of five observations are required to achieve the desired level of IC performance (Jones *et al.* (2001)). However, in most cases, it may not be feasible to wait for the accumulation of sufficient large subgroups, because the users usually want to monitor the process at the start-up stage. The situation may be more serious for general profile monitoring, where there are even larger trail samples required to have an accurate estimate of all the profile parameters.

Hence, many authors had investigated design procedures for traditional control charts with estimated parameters, including Nedumaran and Pignatiello (2001) and Jones (2002). Self-starting methods that update the parameter estimates with new observations and simultaneously check for the OC conditions are developed for situations when sufficient trial samples are unavailable. In the works by Hawkins (1987), Hawkins and Olwell (1998), Quesenberry (1991, 1995), and Sullivan and Jones (2002). Here we propose a self-starting enhancement of the MEWMA control scheme to monitor general linear profiles when the nominal values of the process parameters are not exactly known.

Suppose there are m IC historical samples of size n (as in Phase I analysis). After we obtain $t = m+1, m+2, \cdots$, (including m historical samples and $t-m$ future samples) samples, we have the following statistics

$$\begin{aligned}
\mathbf{z}_t(\beta) &= \sqrt{\frac{t-1}{t}}(\mathbf{X}^\tau\mathbf{X})^{\frac{1}{2}}(\widehat{\beta}_t - \tilde{\beta}_{0,t-1})/\tilde{\sigma}_{0,t-1} \\
\mathbf{z}_t(\sigma) &= \widehat{\sigma}_t^2/\tilde{\sigma}_{0,t-1}^2,
\end{aligned}$$

where $\widehat{\beta}_t$ and $\widehat{\sigma}_t^2$ are defined in Section 3, and $\tilde{\beta}_{0,t-1}$ and $\tilde{\sigma}_{0,t-1}$ are defined in (11) and (12) respectively.

After that, we define the following vector

$$\mathbf{Z_t} = \begin{pmatrix} \mathbf{Z}_t(\beta) \\ \mathbf{Z}_t(\sigma) \end{pmatrix} = \begin{pmatrix} \Phi^{-1}\{f_2[\mathbf{z}_t(\beta); (t-1)n - p]\} \\ \Phi^{-1}\{f_3[\mathbf{z}_t(\sigma); n-p; (t-1)n - p]\} \end{pmatrix}$$

where $f_2(;\nu)$ is the cumulative distribution function of the student-t distribution with ν degrees of freedom and $f_3(;\nu_1;\nu 2)$ is the cumulative distribution function of the F distribution with ν_1 and ν_2 degrees of freedom. When the process is in control, it can be shown that $\mathbf{Z_t}$ is a multivariate normal random vector with a zero mean and an approximate identity covariance matrix. Using a lemma by Basu (Lehmann (1991)), we can show that the sequences of $\mathbf{Z_t}$s are statistically independent. The $\mathbf{Z_t}$ is similar to Q-statistics in Quesenberry (1991) (see also Hawkins (1987) and Hawkins and Olwell (1998)). We can then construct a revised MEWMA chart based on the $\mathbf{Z_t}$ that can update the parameter estimates with new samples and detect the change of parameters simultaneously.

Note that the covariance matrix of the multivariate distribution, $\mathbf{Z_t}$, is not exactly an identity matrix. However, as t increases, this covariance matrix quickly converges to an identity matrix. Hence, we suggest still using the same control limits, L, from the design of the MEWMA chart when the parameters are known to construct such a self-starting chart. Based on an extensive simulation study, we observe that the run-length performance of the proposed self-starting scheme is fairly close to that of the known parameter case. Also, as tabulated in Table 9, the ARL and SDRL performances are rather indifferent to various values of m.

Table 9. The ARL and SDRL of the self-starting MEWMA chart for $m = 10(20)70$

	L=11.87				L=13.34			
	m				m			
	10	30	50	70	10	30	50	70
ARL	202.1	201.6	201.4	200.7	374.1	373.5	373.1	371.4
SDRL	200.8	199.4	199.8	199.2	370.2	370.1	369.5	370.5

The performance of the proposed self-starting chart for monitoring model (2) is demonstrated in Table 10. The case of $m = 30$ IC historical samples and $n = 4$ is considered. Assume that the shift occurs at $t = 30, 50, 100$ and 200 so that the performance assessment can have a broad representation. In total, 50,000 independent series are generated for simulations. Note that any series for which a signal occurs

before sample $(t+1)$ is discarded. $L = 11.87$ are chosen so that the IC ARL is about 200. In Table 10, we notice that the proposed chart performs almost equally well for all values of t when detecting a large shift. The OC ARL is naturally improved as the amount of reference samples increases. However, such an improvement is much more obvious in the case of detecting a small or moderate shift than when detecting a large shift.

Table 10. The ARL performance of the self-starting MEWMA chart for $m = 30$

	δ_1	$t = 30$	$t = 50$	$t = 100$	$t = 200$
	0.2	164.0	141.4	114.8	89.1
	0.4	80.9	47.8	26.9	20.1
	0.6	22.1	12.2	9.3	8.7
A_0	0.8	7.8	6.1	5.6	5.4
$+$	1.0	4.9	4.3	4.1	4.0
$\delta_1\sigma$	1.2	3.7	3.4	3.3	3.2
	1.4	3.1	2.8	2.7	2.7
	1.6	2.7	2.4	2.4	2.4
	1.8	2.4	2.2	2.1	2.1
	2.0	2.2	2.0	1.9	1.9
	0.025	182.6	168.2	151.2	133.7
	0.050	134.2	104.0	70.6	49.5
	0.075	76.2	43.3	24.9	18.9
	0.100	33.0	16.3	11.3	10.3
	0.125	13.7	8.3	7.2	7.0
A_1	0.150	7.2	5.8	5.4	5.2
$+$	0.175	5.2	4.6	4.3	4.3
$\delta_1\sigma$	0.200	4.2	3.8	3.6	3.6
	0.225	3.6	3.3	3.2	3.1
	0.250	3.2	2.9	2.8	2.8
	1.2	111.9	84.6	58.9	42.9
	1.4	44.8	24.3	15.3	12.7
	1.6	17.0	9.6	7.3	7.0
	1.8	8.0	5.6	4.9	4.8
	2.0	5.2	4.1	3.7	3.6
$\delta_1\sigma$	2.2	3.9	3.3	3.0	3.0
	2.4	3.2	2.7	2.6	2.5
	2.6	2.7	2.4	2.3	2.2
	2.8	2.4	2.1	2.0	2.0
	3.0	2.1	1.9	1.9	1.8

10 An Illustration of the Implementation Steps: The DRIE Monitoring Case Revisited

Here, we revisit the DRIE profile monitoring case presented in Section 2 and use that example to demonstrate how to implement the proposed scheme step by step in practice.

We obtain the sample profile data of the DRIE thread, where the (x, y) values are the coordinates obtained from the scanning electron microscope (SEM). After appropriate transformation, we obtain the following quadratic model that can describe the DRIE thread profile:

$$y_{ij} = ax_i^2 + \varepsilon_{ij} \quad i = 1, \cdots, n, \tag{16}$$

where $n = 11$ and $x_i, i = 1, \cdots, 11$ are fixed as equally spaced values, $-2.5, (0.5), 2.5$. Based on the reference sample, the process parameter can be estimated and given by $a = 0.62$ and $\sigma = 0.4$. This model is in the same form as model (1) with $\beta = \left(\beta^{(1)}, \beta^{(2)}, \beta^{(3)}\right) = (1.55, 0.0, 0.62)$. We then apply the proposed MEWMA scheme to monitor the quadratic profile and to detect whether there is any deviation in the process parameters. Detailed implementation steps are as follows.

Step 1. Choose the desired IC ARL and the smoothing constant, λ. Determine the control limit, L, based on p, IC ARL and λ. Here $L = 15.41$ given that $p = 3$, ARL=370 and $\lambda = 0.2$. Consequently, $L\frac{\lambda}{2-\lambda}$ will be 1.71. Then, we can construct the MEWMA control chart as in Figure 2.

Step 2. Start monitoring the process and obtain product observations y_{ij} at fixed values of x_i for $i = 1, \cdots, 11$, sequentially. Whenever obtaining a new sample, compute W_j. Consequently, compute the plot statistic, U_j, in (8) and compare it with control limit $L\frac{\lambda}{2-\lambda}$. In this example, in order to illustrate our proposed diagnostic method more clearly, we assume that $\tau = 5$ and $\beta^{(3)}$ shifts from 0.62 to 0.67 after the fifth sample. The simulated y_{ij} and corresponding U_j for $j = 1, \cdots, 14$ are tabulated in Table 11. From Table 11 and Figure 2, we can see that the MEWMA chart quickly signals a shift at the 14th sample.

Step 3. Then, by looking at the values of $lr(jn, 14n)$ for $j = 0, 1, \cdots, 13$, tabulated in the last column of Table 11, we can find that its maximum occurs at

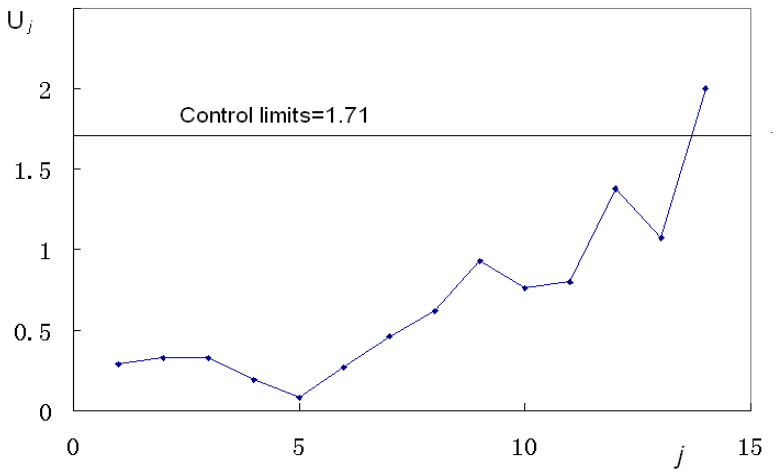

Figure 2. MEWMA chart for the example.

$j = 5$ with $lr(5n, 14n) = 17.78$. This maximum indicates precisely the change-point location, τ, of the shift.

Step 4. Finally, by computing the test statistics, T_{test}, χ^2_{test} and $F^{(i)}_{test}$ for $i = 2, 3$ given in (13), (14) and (15), respectively, we obtain $T_{test} = -0.427$, $\chi^2_{test} = 115.3$, $F^{(2)}_{test} = 0.19$ and $F^{(3)}_{test} = 13.4$. Considering a significant level, $\alpha = 0.05$, it follows that $|T_{test}| < |t(0.025; 9n - 3)| = 1.985$ and $70.8 = \chi^2(0.025; 9n - 3) < \chi^2_{test} < \chi^2(0.975; 9n - 3) = 125.0$, $F^{(2)}_{test} < F_{0.95}(2, 9n - 3, \mathbf{R}) = 3.94$ and $F^{(3)}_{test} > F_{0.95}(2, 9n - 3, \mathbf{R}) = 3.94$, where $t(\alpha; \nu)$ and $\chi^2(\alpha; \nu)$ are the lower percentiles of the Student-t distribution and the χ^2 distribution with ν degrees of freedom, respectively. Hence, our diagnosis concludes that there is a positive shift in the $\beta^{(3)}$ parameter (i.e., a in (16)) after sample 5. Such an increase in the second-order coefficient of the profile indicates an unacceptable positive trench, which may be due to under-etching and the machine settings and conditions need to be re-examined.

Step 5. After correctly identifying the out-of-control parameters and fixing the problem, we will then go back to Step 1 to revise the design of the chart and re-start the monitoring procedure.

11 Conclusions

In this paper, we propose a complete solution to monitor a general linear profile that includes both a polynomial regression and a multiple linear regression model and that can represent many industrial processes. We apply an MEWMA scheme to the transformations of estimated profile parameters as a single chart to monitor both the coefficients and variance of a general linear profile. The proposed scheme can be designed and constructed easily and it has rather satisfactory performance. In particular, three additional features: 1) the variable sampling interval, 2) self-starting function, and 3) parametric diagnostic approach, are provided to enhance the efficiency and effectiveness of the proposed profile monitoring scheme. As demonstrated by the semiconductor DRIE case, the proposed monitoring scheme may be implemented in industrial practice as long as the quality of a process can be characterized by a general linear profile.

Table 11 Data for example with a shift in $\beta^{(3)}$ after the fifth sample.

j	y_{ij}											U_j	lr
0													10.59
1	2.64	2.70	2.10	0.35	0.32	0.35	0.94	0.31	1.15	2.70	4.09	0.29	13.15
2	4.60	2.51	1.28	0.94	-0.09	-0.29	0.96	0.82	1.38	1.66	3.57	0.33	14.43
3	4.21	2.09	1.36	1.18	0.34	-0.67	0.54	-0.03	1.51	2.82	3.70	0.33	14.92
4	3.11	2.46	1.59	0.46	-0.45	0.44	0.05	0.49	1.71	2.79	4.06	0.19	17.07
5	4.14	2.19	1.08	0.47	0.29	-0.08	0.00	0.80	1.05	3.02	4.00	0.08	**17.78**
6	3.64	2.87	0.25	0.51	0.24	0.37	-0.53	0.61	1.40	2.35	4.31	0.27	17.65
7	4.40	2.58	1.25	0.41	0.13	0.19	-0.31	-0.09	1.15	3.42	4.07	0.46	14.09
8	3.92	2.78	1.74	0.10	0.61	-0.99	-0.02	0.30	2.05	2.56	3.61	0.62	13.03
9	4.66	2.97	1.50	1.06	0.12	-0.48	-0.54	0.48	1.21	3.01	3.73	0.93	9.15
10	4.34	2.27	1.31	0.52	0.19	-0.10	0.14	1.07	1.04	3.02	3.86	0.76	11.11
11	3.89	1.82	1.31	0.08	-0.11	0.49	-0.18	-0.28	1.68	2.62	4.12	0.80	11.12
12	4.52	2.43	1.50	0.46	-0.38	-0.61	0.01	1.32	1.20	2.71	4.42	1.38	9.67
13	3.53	2.59	2.57	0.26	0.01	0.13	0.12	0.43	2.02	2.39	4.20	1.07	14.15
14	4.42	3.02	1.93	-0.37	0.30	-0.95	-0.65	1.14	0.76	1.55	3.93	**2.00**	

Appendix

The expression of $lr(tn, kn)$

Based on the change-point model, Mahmoud *et al.* (2005) gave a likelihood ratio test (LRT) statistic for linear profiles in Phase I. This LRT statistic is similar to that of Quandt (1958) and is derived under the assumption that the parameters of the null hypothesis are unknown. Thus, it is not appropriate in Phase II that the in-control parameters are assumed to be known. After k samples have been collected, the logarithm of the likelihood function for them is given by

$$-\frac{1}{2}\sum_{j=1}^{k}\left[n\ln(2\pi\sigma_j^2)+\frac{1}{\sigma_j^2}(\mathbf{Y}_j-\mathbf{X}\beta_j)^\tau(\mathbf{Y}_j-\mathbf{X}\beta_j)\right].$$

If the data are collected under in-control conditions, i.e. under the null hypothesis, the value of the logarithm of the likelihood function is

$$l_0=-\frac{1}{2}\sum_{j=1}^{k}\left[n\ln(2\pi\sigma^2)+\frac{1}{\sigma^2}(\mathbf{Y}_j-\mathbf{X}\beta)^\tau(\mathbf{Y}_j-\mathbf{X}\beta)\right].$$

Assuming a shift occurs after t, then the corresponding maximum value of the logarithm of likelihood is

$$\begin{aligned}l_1=&-\frac{1}{2}\sum_{j=1}^{t}\left[n\ln(2\pi\sigma^2)+\frac{1}{\sigma^2}(\mathbf{Y}_j-\mathbf{X}\beta)^\tau(\mathbf{Y}_j-\mathbf{X}\beta)\right]\\&-\frac{(k-t)n}{2}\ln\left(2\pi\tilde{\sigma}^2_{(t,k)}\right)-\frac{(k-t)n}{2},\end{aligned}$$

where $\tilde{\sigma}^2_{(t,k)}=\frac{(k-t)n-p}{(k-t)n}\tilde{\sigma}^2_{t,k}$ and $\tilde{\sigma}^2_{t,k}$ is defined in (12). Then, the generalized likelihood ratio statistic is given by

$$\begin{aligned}lr(tn,kn)&=-2(l_0-l_1)\\&=\sum_{j=t+1}^{k}\frac{1}{\sigma^2}(\mathbf{Y}_j-\mathbf{X}\beta)^\tau(\mathbf{Y}_j-\mathbf{X}\beta)-(k-t)n\Big[\ln\Big(\frac{\tilde{\sigma}^2_{(t,k)}}{\sigma^2}\Big)+1\Big].\end{aligned}$$

References

Aparisi, F. (1996), "Hotelling's T^2 Control Chart with Variable Sampling Intervals," *International Journal of Production Research*, 39, 3127-3140.

Calzada, M. E., Scariano, S. M. and Chen, G. (2004), "Computing Average Run Lengths for the Maxewma Chart," *Communications in Statistics: Simulation and Computation*, 33, 489-503.

Chen, G., Cheng, S. W. and Xie, H. (2001), "Monitoring Process Mean and Variability With One EWMA Chart," *Journal of Quality Technology*, 33, 223-233.

Chengular, I. N., Arnold, J. C. and Reynolds, M. R. Jr. (1993), " Variable Sampling Interval for Multiparameter Shewhart Charts," *Communications in Statistics: Theory and Methods*, 18, 1769-1792.

Croarkin, C. and Varner, R. (1982), "Measurement Assurance for Dimensional Measurements on Integrated-Circuit Photomasks," NBS Technical Note 1164, U.S. Department of Commerce, Washington, D.C., USA.

Csorgo, M. and Horvath, L. (1997), *Limit Theorems in Change-Point Analysis*, John Wiley, New York.

Gan, F. F. (1995), "Joint Monitoring of Process Mean and Variance Using Exponentially Weighted Moving Average Control Charts, *Technometrics*, 37, 446-453.

Gupta, S., Montgomery, D. C., and Woodall, W. H. (2006), "Performance Evaluation of Two Methods for Online Monitoring of Linear Calibration Profiles," *International Journal of Production Research*, in press.

Hawkins, D. M. (1987), "Self-Starting CUSUM Charts for Location and Scale," *The Statistician*, 36, 299-315.

Hawkins, D. M. and Olwell, D. H. (1998), *Cumulative Sum Charts and Charing for Quality Improvement*, Springer-Verlag, New York, NY.

Hawkins, D. M. and Zamba, K. D. (2005), "Statistical Process Control for Shifts in Mean or Variance Using a Change-Point Formulation," *Technometrics*, 47, 164-173.

Jensen, D. R., Hui, Y. V. and Ghare, P. M. (1984), "Monitoring an Input-Output Model for Production. I: The Control Charts," *Management Science*, 30, 1197-1206.

Jones, L. A. (2002), "The Statistical Design of EWMA Control Charts with Estimated Parameters," *Journal of Quality Technology*, 34, 277-288.

Jones, L. A., Champ, C. W. and Rigdon, S. E. (2001), "The Performance of Exponentially Weighted Moving Average Charts with Estimated Parameters," *Technometrics*, 43, 156-167.

Jones, L. A., Champ, C. W. and Rigdon, S. E. (2004), "The Run Length Distribution of the CUSUM with Estimated Parameters," *Journal of Quality Technology*, 36, 95-108.

Kang, L. and Albin, S. L. (2000), "On-Line Monitoring When the Process Yields a Linear Profile," *Journal of Quality Technology*, 32, 418-426.

Kim, K., Mahmoud, M. A. and Woodall, W. H. (2003), "On the Monitoring of Linear Profiles," *Journal of Quality Technology*, 35, 317-328.

Kotz, S., Balakrishnan, N. and Johnson, N. L. (2000), *Continuous Multivariate Distributions, 2nd edn*, Wiley-Interscience, New York.

Lawless, J. F., Mackay, R. J., and Robinson, J. A. (1999), "Analysis of Variation Transmission in Manufacturing Processes-Part I," *Journal of Quality Technology*, 31, 131-142.

Lehmann, E. L. (1991), "*Theory of Point Estimation*." Wadsworth&Brooks, Pacific Grove, California.

Lowry, C. A., Woodall, W. H., Champ, C. W. and Rigdon, S. E. (1992), "Multivariate Exponentially Weighted Moving Average Control Chart," *Technometrics*, 34, 46-53.

Lucas, J. M. and Saccucci, M. S. (1990), "Exponentially Weighted Moving Average Control Scheme Properties and Enhancements," *Technometrics*, 32, 1-29.

Mahmoud, M. A. and Woodall, W. H. (2004), "Phase I Analysis of Linear Profiles with Calibration Applications," *Technometrics*, 46, 380-391.

Mahmoud, M. A., Parker, P. A., Woodall, W. H., and Hawkins, D. M. (2005), "A Change Point Method for Linear Profile Data," to appear in *Quality and Reliability Engineering International*.

May, G. S., Huang, J., and Spanos, C. J. (1991), "Statistical experimental design in plasma etch modeling," *IEEE Transactions on Semiconductor Manufacturing*, 4, 83-98.

McAuley, S. A., Ashraf, H., Atabo, L., Chambers, A., Hall, S., Hopkins, J., and Nicholls, G. (2001), "Silicon Micromachining Using a High-Density Plasma Source," *Journal of Physics D-Applied Physics*, 34, 2769-2774.

Mestek, O., Pavlik, J., and Suchanek, M. (1994), "Multivariate Control Charts: Control Charts for Calibration Curves," *Journal of Analytical Chemistry*, 350, 344-351.

Molnau, W. E., Runger, G. C., Montgomery, D. C., Skinner, K. R., Loredo, E. N. and Prabhu, S. S. (2001), " A program for ARL Calculation for Multivariate EWMA Charts," *Journal of Quality Technology*, 33, 515-521.

Montgomery, D. C. (2004), *Introduction to Statistical Quality Control,* 5^{th} *ed*, John Wiley & Sons, New York, NY.

Nedumaran, G. and Pignatiello, J. J. JR. (2001), "On Estimating $\bar{X}$ Control Chart Limits," *Journal of Quality Technology*, 33, 206-212.

Nishina, K. (1992), "A Comparison of Control Charts From the Viewpoint of Change-Point Estimation," *Quality and Reliability Engineering International*, 8, 537-541.

Pignatiello, J. J. Jr. and Samuel, T. R. (2001), "Estimation of the Change Point of a Normal Process Mean in SPC Applications," *Journal of Quality Technology*, 33, 82-95.

Prabhu, S. S. and Runger, G. C. (1997), "Designing a Multivariate EWMA Control Chart," *Journal of Quality Technology*, 29, 8-15.

Quandt, R. E. (1958), "The Testing of the Parameters of a Linear Regression System Obeys Two Separate Regimes," *Journal of American Statistical Association*, 53, 873-880.

Quesenberry, C. P. (1991), "SPC Q Charts for Start-up Processes and Short or Long Runs," *Journal of Quality Technology*, 23, 213-224.

Quesenberry, C. P. (1993), "The Effect of Sample Size on Estimated Limits for $\bar{X}$ and X Control Charts, *Journal of Quality Technology*, 25, 237-247.

Quesenberry, C. P. (1995), "On Properties of Q Charts for Variables," *Journal of Quality Technology*, 27, 184-203.

Reynolds, M. R. Jr. (1989), "Optimal Variable Sampling Interval Control Charts," *Sequential Analysis*, 8, 361-379.

Rauf, S., Dauksher, W. J., Clemens, S. B., and Smith, K. H. (2002), "Model for a Multiple-Step Deep Si Etch Process," *Journal of Vacuum Science and Technology A*, 20, 1177-1190.

Reynolds, M. R. Jr., Amin, R. W., and Arnold, J. C. (1990), "CUSUM Charts with Variable Sampling Intervals," *Technometrics*, 32, 371-384.

Reynolds, M. R. Jr., Amin, R. W., Arnold, J. C., and Nachlas, J. A. (1988) "$\bar{X}$ Charts with Variable Sampling Intervals," *Technometrics*, 30, 181-192.

Reynolds, M. R. Jr. and Arnold, J. C. (2001), "EWMA Control Charts with Variable Sample Sizes and Variable Sampling Intervals," *IIE Transactions*, 33, 66-81.

Reynolds, M. R. Jr. and Kim, K. (2005a), "Multivariate Monitoring of the Process Mean Vector With Sequential Sampling," *Journal of Quality Technology*, 37, 149-162.

Reynolds, M. R. Jr. and Kim, K. (2005b), "Monitoring Using an MEWMA Control Chart with Unequal Sample Sizes," *Journal of Quality Technology*, 37, 267-281.

Reynolds, M. R. Jr. and Stoumbos, Z. G. (2001), "Monitoring the Process Mean and Variance Using Individual Observations and Variable Sampling Intervals," *Journal of Quality Technology*, 33, 181-205.

Reynolds, M. R. Jr. and Stoumbos, Z. G. (2005), "Should Exponentially Weighted Moving Average and Cumulative Sum Charts Be Used With Shewhart Limits," *Technometrics*, 47, 409-424.

Rigdon, S. E. (1995a), "A Double Integral Equation for the Average Run Length of a Multivariate Exponentially Weighted Moving Average Control Chart," *Statistics and Probability Letters*, 24, 365-373.

Rigdon, S. E. (1995b), "An Integral Equation for the In-Control Average Run Length of a Multivariate Exponentially Weighted Moving Average Control Chart" *Journal of Statistical Computation and Simulation*, 52, 351-365.

Runger, G. C. and Montgomery, D. C. (1993), "Adaptive Sampling Enhancements for Shewhart Control Charts," *IIE Transactions*, 25, 41-51.

Runger, G. C. and Prabhu, S. S. (1996), "A Markov Chain Model for the Multivariate Exponentially Weighted Moving Averages Control Chart," *Journal of American Statistical Association*, 91, 1701-1706.

Stover, F. S. and Brill, R. V. (1998), "Statistical Quality Control Applied to Ion Chromatography Calibrations," *Journal of Chromatography A*, 804, 37-43.

Sullivan, J. H. and Jones, L. A. (2002), "A Self-Starting Control Chart for Multivariate Individual Observations," *Technometrics*, 44, 24-33.

Woodall, W. H., Spitzner, D. J., Montgomery, D. C. and Gupta, S. (2004), "Using Control Charts to Monitor Process and Product Quality Profiles," *Journal of Quality Technology*, 36, 309-320.

Zhou, R., Zhang, H., Hao, Y. and Wang, Y. (2004), "Simulation of the Bosch Process with a String-Cell Hybrid Method," *Journal of Micromechanics and Microengineering*, 14, 851-858.

Zou, C., Zhang, Y. and Wang, Z. (2006), "Control Chart Based on Change-Point Model for Monitoring Linear Profiles," to appear in *IIE Transactions*.